

# First results from LArRI: A new setup for Liquid Argon Refractive Index measurement

**Alice Campani,<sup>a,b,\*</sup> Bianca Bottino,<sup>a,b</sup> Ruggero Caravita,<sup>c</sup> Simone Copello,<sup>d</sup> Federico Ferraro,<sup>e</sup> Alessio Caminata,<sup>b</sup> Massimo Cariello,<sup>b</sup> Sergio Di Domizio,<sup>a,b</sup> Lea Di Noto,<sup>a,b</sup> Paolo Musico,<sup>b</sup> Marco Pallavicini,<sup>a,b</sup> Silvia Repetto,<sup>a,b</sup> Giuliano Sobrero<sup>b</sup> and Gemma Testera<sup>b</sup>**

<sup>a</sup>*Dipartimento di Fisica, Università degli studi di Genova  
Via Dodecaneso 33, 16146, Genova, Italia*

<sup>a</sup>*Istituto Nazionale di Fisica Nucleare, Sezione di Genova,  
Via Dodecaneso 33, 16146, Genova, Italia*

<sup>c</sup>*Trento Institute for Fundamental Physics and Applications,  
Via Sommarive 14, 38123, Povo (TN), Italia*

<sup>d</sup>*Istituto Nazionale di Fisica Nucleare, Sezione di Pavia,  
Via Bassi 6, 27100, Pavia, Italia*

<sup>e</sup>*Istituto Nazionale di Fisica Nucleare, Laboratori Nazionali del Gran Sasso  
Via Accitelli 22, 67100, Assergi (AQ), Italia*

*E-mail:* [alice.campani@ge.infn.it](mailto:alice.campani@ge.infn.it)

Liquid Argon (LAr), widely used as active target in neutrino and dark matter experiments, is a scintillator with a light yield of about 40 photons/keV, an attenuation length of the order of meters and a scintillation peak at 128 nm. Adding small amounts of dopant, i.e. xenon, (around 10 ppm) allows to shift the scintillation center to 178 nm without spoiling the light yield. The longer wavelength simplifies the light detection thereby impacting the development of imaging systems. A precise knowledge of LAr optical properties in the VUV range is essential to improve the performance of liquid argon-based experiments. Besides, the refractive index is a crucial parameter for the development of imaging systems. LArRI (Liquid Argon Refractive Index) aims at a direct measurement of LAr refractive index in the VUV spectrum using an interferometric technique. This approach relies on the comparison of two interference patterns, created in vacuum and in liquid, respectively, and measured by cryogenic silicon photomultipliers. We obtain a source of monochromatic, coherent light using a mercury lamp with emission peaks at 254 and 184 nm. In this Article, we present the results of the commissioning stage of the experiment, including our first measurements with cryogenic liquids.

*42nd International Conference on High Energy Physics (ICHEP2024)  
18-24 July 2024  
Prague, Czech Republic*

---

\*Speaker

## 1. Introduction

Liquid Argon (LAr) is widely used in particle physics [1], including neutrino experiments [2, 3] and dark matter searches [4, 5]. Among the main reasons for a wide use of LAr - besides its scintillation properties - we have its low cost, high availability and the possibility of purification. The light yield is about 40 photons/keV and the scintillation emission peak is 128 nm, but Xenon-doping in small amounts ( $\sim 10$  ppm) can be employed to guarantee an increased light collection and signal uniformity, shifting the peak to 175 nm [6]. The longer wavelength simplifies signal detection and allows the development of optical systems, such as lenses for Xe-doped LAr imaging [7].

As a result, measuring LAr optical properties in the VUV range is crucial for the success of experiments. In particular, LArRI (Liquid Argon Refractive Index) has the primary goal of making a direct measurement of LAr refractive index at  $\sim 175$  nm. Other interesting results that can be achieved with the same setup include measuring the dispersion relation, performing the same measurement at different wavelengths, the measurement of the attenuation length and the characterization of optical properties of other noble gases, including Xenon.

## 2. Measurement strategy

The key idea of LArRI experiment is to measure the liquid argon refractive index with a differential interferometric approach, i.e. by comparing the diffraction patterns generated when light propagates in vacuum and liquid argon by means of a diffraction grating. Indirect measurements of the LAr refractive index using the group velocity are also possible [8], though the precision that can be achieved with this approach is limited. Given the low temperature requirement and the wavelengths in the VUV range, an interferometric approach is the most appropriate. In general, the position of the diffraction peaks generated by the grating depends on the wavelength, which is shifted from its value in vacuum,  $\lambda_0$ , to  $\lambda_L = \frac{\lambda_0}{n}$  when the grating is immersed in LAr,  $n$  being the refractive index we want to measure. This means that diffraction maxima are located at

$$d \sin \theta_0 = \lambda_0 \quad (\text{in vacuum}) \quad (1)$$

$$d \sin \theta_L = \lambda_L \quad (\text{in LAr}) . \quad (2)$$

In order to generate the diffraction patterns, we need to produce a source of coherent and monochromatic light with wavelength close to 175 nm. In LArRI we employ a low pressure mercury lamp with two emission peaks at 184.9 nm and 253.7 nm. This is coupled to a custom built optical setup to deliver monochromatic coherent light into the cryogenic chamber. The light signal is collected using silicon photomultipliers (SiPMs) operated at cryogenic temperatures. Further details on the setup including both the *cold part*, that is maintained at low temperature by means of a cryostat, and the *warm part* that sits at room temperature are provided in the next section.

## 3. Experimental apparatus

The core of LArRI experimental setup consists in two parts:

- the warm part, consisting in the optical apparatus to generate coherent, monochromatic light near 175 nm, the DAQ system and the SiPMs electronics;

- the cold part, including a cryostat to thermalize and maintain the system at low temperatures, a cylindrical chamber that can be evacuated or filled with cryogenic liquids and the light detection system, i.e. the SiPMs that are located onto a movable stand to register the diffraction pattern in the two configurations, vacuum and LAr.

To compress the apparatus and reduce the chamber dimensions, the diffraction peaks are not scanned horizontally, i.e. on the side opposite to that of the grating, but vertically, along the chamber. A schematic of the experimental setup is reported in Fig. 1.

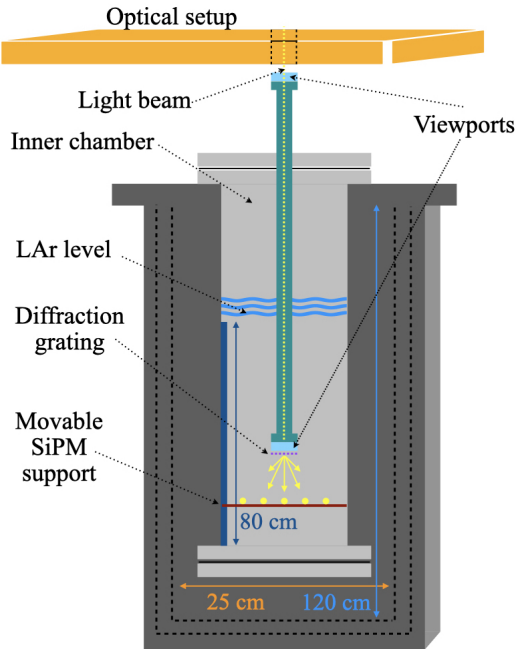


**Figure 1:** Scheme of LArRI experimental setup. The optical setup is assembled onto a breadboard (orange) positioned on top of the cryostat (dark grey). A hole in the breadboard connects the collimated light beam with the vertical tube (green) entering the cryogenic chamber (grey). This is enclosed by two  $\text{MgF}_2$  viewports (light-blue) and kept in vacuum to minimize the signal loss due to UV photons absorption. The diffraction grating (purple) is suspended below the innermost viewport and faces the movable stand (brown) where the SiPMs to collect light are positioned. The dimensions of the innermost cryostat chamber as well as the vertical range the motor can explore are also indicated.

### 3.1 Warm part of the detector: optical setup, DAQ and electronics

As shown in Fig. 1, all the optical system from the mercury lamp to the launch mirrors is assembled on a breadboard located on top of the cryostat. Being in air, we have about 50% light loss at 184.9 nm. From left to right, we find the following elements:

- the light source, i.e. a low pressure mercury lamp with several emission peaks positioned in a range from 180 to 600 nm, the most intense ones being at 184.9 and 253.7 nm, respectively<sup>1</sup>, the former is our proxy for the LXe-doped scintillation peak;
- a tunable slit to gain spatial coherence, a convergent lens to produce plane waves and a  $\text{CaF}_2$  prism to separate wavelengths;

<sup>1</sup>The power ratio is  $\sim 1:5$

- at a distance of  $\sim$ 40 cm two launch mirrors to inject the light beam into the chamber, a hole in the breadboard is aligned with the vertical tube that sends the light towards the grating.

The SiPMs electronics [9] includes two custom-made front end boards positioned outside the cryostat. They supply bias voltage to the SiPMs and integrate their current signal ( $\tau = 100$  ms). The data acquisition system consists of a Teledyne Lecroy scope. We acquire 100-ms long windows at a typical rate of 2-10 Hz. We average them to extract the luminosity sample used for the analysis.

### 3.2 Cold part of the detector: LArRI chamber

The cold part of the apparatus includes the cryostat, the inner chamber, that can be either evacuated or filled with cryogenic liquids, and the vertical tube that brings in the collimated light beam coming from the top. The vertical tube is enclosed by two  $\text{MgF}_2$  viewports and kept in vacuum to reduce the signal loss due to absorption of UV photons. The diffraction grating is suspended below the innermost viewport and is made of Aluminum deposited on a thin fused silica substrate. The pitch is 723 nm. The light detectors are 5 Hamamatsu (S13370-3075CN)  $3 \times 3 \text{ mm}^2$  UV-sensitive SiPMs. One of them is positioned at the center of the movable stand and employed for the alignment procedure (see Sec. 3.2.1). The remaining 4 SiPMs are symmetrically mounted on each side to detect light coming from the diffraction peaks. The support hosting the SiPMs is secured onto a motor by VacuumFab<sup>2</sup> that is capable of operating both in vacuum and immersed in cryogenic liquids. To monitor the temperature and liquid level, the setup features 3 resistive temperature devices positioned at different heights inside the chamber.

#### 3.2.1 Light source-cold chamber alignment procedure

Since the 184.9 nm peak has very low intensity, it is impossible to guarantee a proper alignment of the light beam and the grating/light collection system relying on the lamp signal alone. We developed a two-steps alignment procedure, using an additional 402.9 nm laser source. First, we align the 184.9 nm line and the laser using a movable CCD camera. Then, we align the laser with the SiPM located at the center of the movable stand. This is done moving the SiPMs support from top to bottom of the chamber in order to guarantee the maximum achievable SNR for the entire scan. With our tests, we confirmed the SiPM signal is constant within 30% and reproducible in the upward and downward directions.

## 4. Data analysis

The first step of the data analysis focuses on extracting the 8 luminosity maxima corresponding to the  $M_{1,2}$  diffraction peaks intercepted by each of the 4 lateral SiPMs. The motor moves at constant speed and its displacement is synchronized with the trigger. Thus, we can use the position of the motor at the beginning (top) and end (bottom) of the scan (chamber) to identify the vertical position of the diffraction peaks for each light detector. This is typically done twice in the analysis chain: first on the vacuum scan and then on the liquid (argon) one.

The core of the analysis is the subsequent fit, through which we extract a measurement of the cryogenic liquid (LAr) refractive index by combining the results of two scans (8+8 data points).

<sup>2</sup><https://www.vacuumfab.com/prodotti>

The choice of a simultaneous fit is driven by the assumption that geometrical parameters are the same in vacuum and liquid and aims at reducing the impact of systematic effects produced by non idealities of the setup. In a reference frame where  $z$  indicates the axis perpendicular to the grating, i.e. the motor axis, and  $x$  the axis jointed to the movable SiPM stand, the expected vertical position of each peak is:

$$z_{exp_i} = \frac{(x_i + x_0) \cdot \cos \theta_s}{\tan \left[ \arcsin \left( \frac{m\lambda}{an} \right) \right]} - (x_i + x_0) \cdot \sin \theta_s - z_0 \quad (3)$$

where  $x_i$  are the positions of the 16 diffraction peaks along  $x$ ,  $m = 1, 2$  and the free parameters are:

- $x_0$  that accounts for a possible offset on the position of the SiPMs on the movable support,
- $\theta_s$  which is the complement of the angle between the motor axis and the movable stand,
- $a$  that indicates the grating period,
- $n$ , the liquid (argon) refractive index, ruling the diffraction pattern contraction in liquid,
- $z_0$  that refers to the initial position of the movable support along the motor axis.

Fitting the peaks we extract an estimate of the parameter of interest,  $n$ , and the nuisance parameters.

## 5. First results

For the sake of clarity, from now on for each result we will indicate the number of measurements employed to extract it as  $a \times b$ , where  $a$  indicates the number of scans performed in vacuum and  $b$  the number of scans with LArRI chamber filled with liquid where, unless otherwise specified, this means LAr. Each scan in vacuum is fit against each scan in liquid to extract an estimate of  $n$ . The final value is obtained averaging the outcome of single fits.

### 5.1 Validation of the analysis strategy

From Eq. 3, it is evident that  $\lambda$  and  $n$  are degenerate. Given two scans at different wavelengths, but in the same medium, e.g. vacuum, one can employ the same strategy outlined above and extract a contraction factor equal to the ratio between the two wavelengths, i.e.  $n = \frac{\lambda_2}{\lambda_1}$ . We used this to make consistency checks of our method: we performed the analysis using 2 laser scans at 402.9 nm against 5 scans at 253.7 nm, i.e. the most intense line of our lamp, plus their average. We measured the two wavelengths independently with a spectrometer and, comparing the expected contraction factor with each fit, we observe a compatibility within few parts per thousand.

### 5.2 First measurements in cryogenic liquids

We performed our first measurements in liquid using nitrogen instead of argon and measured the refractive index both with the laser and the 253.7 nm line of the mercury lamp. We obtain  $n_{LN_2}(253.7 \text{ nm}) = (1.24 \pm 0.01)$  by averaging the result of the analysis of 8 x 8 scans, and  $n_{LN_2}(402.9 \text{ nm}) = (1.24 \pm 0.01)$  from two independent measurements.

We extract our preliminary results in liquid argon with scans performed using only 2 lateral SiPMs, since we found that 2 of our light detectors were not functioning anymore. The results of a

simultaneous fit of 4+4 diffraction maxima are listed below:

$$n_{\text{LAr}}(402.9 \text{ nm}) = (1.24 \pm 0.01) \text{ with 2x1 scans} \quad (4)$$

$$n_{\text{LAr}}(253.7 \text{ nm}) = (1.24 \pm 0.01) \text{ with a single measurement} \quad (5)$$

$$n_{\text{LAr}}(184.9 \text{ nm}) = (1.29 \pm 0.05) \text{ with 2x1 scans} \quad (6)$$

where we assume conservative uncertainties, taking into account the dominant effect of systematics due to non-idealities in the grating and in the geometry of the setup.

## 6. Conclusive remarks

Following the setup commissioning, LArRI is fully operational since 2023 and we were able to acquire our first scans in vacuum and cryogenic liquids, i.e. nitrogen and argon. We developed and validated a robust analysis strategy. Our goals include performing dedicated studies to increase our precision in the estimate of systematic effects (optical system, grating, ...), improving our measurement at 184.9 nm and repeating the measurement in LAr with the full set of light detectors.

## References

- [1] W. M. Bonivento and F. Terranova, [arXiv:2405.01153 [physics.ins-det]].
- [2] B. Abi *et al.* [DUNE], Eur. Phys. J. C **80** (2020) no.10, 978 doi:10.1140/epjc/s10052-020-08456-z [arXiv:2006.16043 [hep-ex]].
- [3] P. A. Machado, O. Palamara and D. W. Schmitz, Ann. Rev. Nucl. Part. Sci. **69** (2019), 363-387 doi:10.1146/annurev-nucl-101917-020949 [arXiv:1903.04608 [hep-ex]].
- [4] A. Zani [DarkSide-20k], JINST **19** (2024) no.03, C03058 doi:10.1088/1748-0221/19/03/C03058 [arXiv:2402.07566 [physics.ins-det]].
- [5] S. Viel [DEAP-3600], PoS **TAUP2023** (2024), 075 doi:10.22323/1.441.0075
- [6] A. Neumeier, T. Dandl, T. Heindl, A. Himpisl, L. Oberauer, W. Potzel, S. Roth, S. Schönert, J. Wieser and A. Ulrich, EPL **109** (2015) no.1, 12001 doi:10.1209/0295-5075/109/12001 [arXiv:1511.07723 [physics.ins-det]].
- [7] M. Vicenzi, doi:10.15167/vicenzi-matteo\_phd2023-01-20
- [8] M. Babicz, S. Bordoni, A. Fava, U. Kose, M. Nessi, F. Pietropaolo, G. L. Raselli, F. Resnati, M. Rossella and P. Sala, *et al.* JINST **15** (2020) no.09, P09009 doi:10.1088/1748-0221/15/09/P09009 [arXiv:2002.09346 [physics.ins-det]].
- [9] M. Cariello, B. Bottino, A. Campani, R. Caravita, S. Copello, F. Ferraro, A. Caminata, S. Di Domizio, L. Di Noto and P. Musico, *et al.* Nucl. Instrum. Meth. A **1068** (2024), 169756 doi:10.1016/j.nima.2024.169756